

25th Machining Innovations Conference for Aerospace Industry 2026 (MIC 2026),
4th and 5th February 2026, Hannover, Germany

Experimental Framework for Investigating Manual Drilling in Aircraft Assembly

Malte Flehmke^{a,*}, Ferdinand Fritz^{a,b}, Sascha Fangmann^c, Jan H. Dege^a

^aInstitute of Production Management and Technology (IPMT), Hamburg University of Technology (TUHH), Denickestr. 17, 21073 Hamburg, Germany

^bAirbus Operations GmbH, Kreetzslag 10, 21129 Hamburg, Germany

^cAirbus Operations GmbH, Airbus-Allee 1, 28199 Bremen, Germany

* Corresponding author. Tel.: +49 40 42878 3494; E-mail address: malte.flehmke@tuhh.de

Abstract

In aircraft structural assembly, a substantial share of rivet holes is drilled manually using handheld machines. In contrast to semi-automatic drilling machines, operations with handheld tools are subject to process-inherent parameter variations such as fluctuations in feed force and differences in tool alignment, both of which strongly influence hole quality and tool wear. Moreover, handheld drilling machines typically lack integrated sensing capabilities, further complicating process monitoring and quality assurance. To address these challenges, a dedicated experimental test rig for manual drilling is developed and tested. The setup enables systematic investigation of manual drilling operations under controlled conditions, incorporating external sensors to capture key process signals such as feed force, spindle speed, torque and feed travel. Based on these measurements, derived parameters such as feed rate and drilling time can be analyzed to study their relationship to hole exit quality, particularly delamination in carbon fiber reinforced polymer (CFRP) material. Initial investigations using Random Forest classification and permutation importance to identify significant process characteristics demonstrate that higher feed rates right before tool exit correlate with increased delamination, consistent with the findings from automated drilling research. The results further reveal a strong influence of operator-induced variability and tool wear on the measured process parameters, with feed force variations exceeding 40 N within individual drilling operations. This emphasizes the need for systematic understanding of human-machine interactions in manual drilling and motivates the development of monitoring and assistance systems capable of compensating operator-induced variations. The presented experimental framework provides a foundation for quantitative analysis of manual drilling behavior and serves as a data-driven basis for future work on process monitoring, anomaly detection, and operator feedback control.

© 2026 The Authors. Published by SSRN, available online at <https://www.ssrn.com/link/MIC-2026.html>

This is an open access article under the CC BY-NC-ND license (<http://creativecommons.org/licenses/by-nc-nd/4.0/>)

Peer review statement: Peer-review under responsibility of the scientific committee of the 25th Machining Innovations Conference for Aerospace Industry 2026

Keywords: Aircraft Assembly, Manual Drilling, Experimental Test Rig, Process Monitoring, Rivet Hole Quality, Integrated Sensing, CFRP Drilling

1. Introduction

The development of future aircraft is driven by the demand for lighter, more efficient, and more sustainable designs [1]. Fiber-reinforced polymers (FRPs), particularly carbon fiber reinforced polymers (CFRP), play a key role in this evolution [2]. Their anisotropic material properties enable tailored

structural performance and significant weight reductions compared to metals [3], directly lowering fuel consumption and greenhouse gas emissions [2]. Although CFRP components are more expensive to manufacture, cost premiums of up to 5,000 € per kilogram of weight saved are considered acceptable in aerospace applications [4]. One of the main contributing factors to the increased cost are manual drilling operations.

© 2026 The Authors. Published by SSRN, available online at <https://www.ssrn.com/link/MIC-2026.html>

This is an open access article under the CC BY-NC-ND license (<http://creativecommons.org/licenses/by-nc-nd/4.0/>)

Peer review statement: Peer-review under responsibility of the scientific committee of the 25th Machining Innovations Conference for Aerospace Industry 2026.

Nomenclature

B	number of decision trees in Random Forest
b	test material thickness
D_0	hole diameter
D_{max}	maximum diameter of the delamination zone
D_t	tool diameter
E_{OOB}	baseline OOB error rate
$E_{OOB}^{(j)}$	OOB error with feature j permuted
F_d	delamination factor
$F_{d,max}$	maximum allowed delamination factor
F_f	feed force
f	feed
f_s	sampling frequency
b	material thickness
h_B	drilling height
I_j	importance score of feature j
n	spindle speed
n_{exp}	experimentally used spindle speed
N	number of samples
N_t	number of holes drilled with respective tool
N_{OOB}	number of samples not included in bootstrap sample
p	overall number of features
l_f	feed travel
M_c	cutting torque
T_b	individual decision tree
t	time
x	feature vector
X_j	feature j
y	true label
\hat{y}	predicted label
y_i	true label of sample i
φ_B	drilling rig angle

Drilling is one of the most critical and costly machining processes in aircraft assembly, as riveted joints require vast numbers of high-precision holes [5]. The global aircraft industry produces roughly 300 million rivet holes annually, with around 250,000 per medium-sized aircraft. Across all production sites, approximately 30 % of these holes are drilled manually. Manual drilling remains essential in areas with limited accessibility [4] but is prone to quality deviations such as diameter inaccuracies, fiber breakout, and delamination [6,7]. These defects can compromise structural integrity of the aircraft and lead to costly rework [4]. In automated drilling, the process parameters are generally very well known. Therefore, a prediction of the hole quality and specifically the delamination is possible based on empirical data [8-10] or modelling approaches [11-14]. Compared to automated or semi-automatic processes, manual operations are subject to inherent fluctuations in feed force and differences in tool alignment resulting primarily from the human-applied force control that governs the manual drilling process. Both factors, varying feed force and non-consistent tool alignment, strongly influence hole quality and tool wear. Consequently, the operational challenge for operators lies in rapidly decreasing the feed force at the chisel edge breakthrough, which demands a high degree of dexterity and experience. As a result, robust process reliability with respect to delamination prevention cannot be inherently

guaranteed in manual drilling [4]. Demonstrating the ability to correlate process data with hole quality, especially delamination, during manual drilling remains an open challenge. Handheld drilling devices typically lack integrated sensing capabilities, complicating process monitoring and quality assurance. Due to the high process variability resulting from a high operator dependence, error rates are often higher during manual drilling when compared to automatic or semi-automatic drilling. High employee turnover and insufficient training of new, non-specialist staff are known to increase error rates further. Current solution approaches often rely on dampers [4] and linear motors [15] to guide the operator by slowing down the feed during workpiece exit, thus reducing exit delamination. The authors in [6] developed an ultrasonically actuated drilling machine leading to a reduction in shakiness and a reduction of the overall feed force. Nevertheless, current approaches interfere directly with the operator's work process, which leads to low acceptance and limited practical use. On the other hand, research focusing specifically on manual drilling is scarce in the literature. Force profiles, ergonomic factors, and the variability influenced by the machine operator's experience are currently underexplored. To address this issue, a dedicated experimental test rig for manual drilling was developed, which facilitates systematic investigation of the process behavior under controlled conditions. Equipped with external sensors to capture key parameters such as feed, speed, and process forces, the setup provides a foundation for collecting extensive data of the manual drilling process. The measurement data provides a baseline for deeper process understanding, the development of monitoring strategies, and future implementation of operator assistance systems aimed at improving drilling quality. The experimental setup is used to determine the parameters that most accurately predict the delamination damage on drill hole exit. Final results are interpreted in context of the existing literature on automatic drilling of CFRP.

Sect. 2 describes the underlying methodology and proposes a test rig for conducting manual drilling experiments. In Sect. 3 the experimental procedure and first results are presented. An evaluation of the data using Random Forests and permutation importance is presented in Sect. 4, determining the correlation between exit delamination and measurement data. Finally, in Sect. 5 the results are summarized and an outlook on further research is given.

2. Methodology and Experimental Test Rig

In this section, the test rig for manual drilling is presented, enabling systematic studies under controlled environmental conditions. The setup allows integration of sensors to capture key process signals such as feed, spindle speed, and forces, providing a basis for future research on process understanding, monitoring, and anomaly detection for varying ergonomic situations.

2.1. Mechanical configuration

The mechanical setup is presented in Fig. 1. The test rig is mounted on a drilling rack which can be adjusted in height and angle. Thus, the test rig can be modified to represent different ergonomic situations. The frame includes a simple clamping fixture with two adjustable clamps, as well as upper and lower stops to secure the test specimen and prevent the workpiece from rotating during drilling. On the front side of the test rig, an opening is provided for a drilling guide, whose bushing can be adapted to the respective tool diameter. To maintain realistic conditions and avoid tilting, the guide has to be held in place manually despite the fixture. Because drilling CFRP requires effective dust extraction, which in practice often demands additional personnel, an integrated vacuum system was added to the test setup. A custom nozzle for the vacuum is mounted to the frame of the test rig. External sensors are added to the frame.

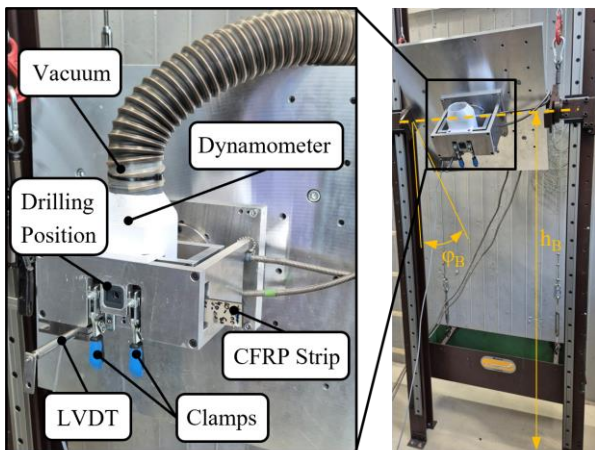


Fig 1. Individual components of the test rig for manual drilling; The test rig is mounted on a height adjustable rack enabling the adjustment of drilling height h_B and drilling angle ϕ_B .

A Kistler dynamometer type 9271A is mounted underneath the frame to measure process forces and torques. To measure depth of cut, a linear variable differential transformer (LVDT) HBM WA100 is mounted to the side of the frame. Additionally, a hall sensor Infineon TLE4905L is mounted to the drilling machine itself, see Fig. 2. Two magnets are embedded into a rotating ring on the drill chuck enabling the measurement of the spindle speed. An additional pull-up resistor ensures data integrity on the digital output.

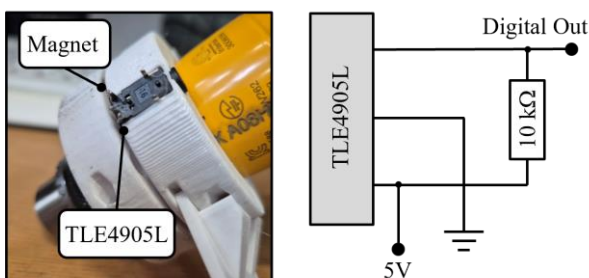


Fig 2. Measurement setup for spindle speed

2.2. Instrumentation and control configuration

To capture the relevant process parameters during drilling, a comprehensive measurement setup was developed that enables synchronized acquisition of spindle speed, feed motion, and process force signals, see Fig. 3.

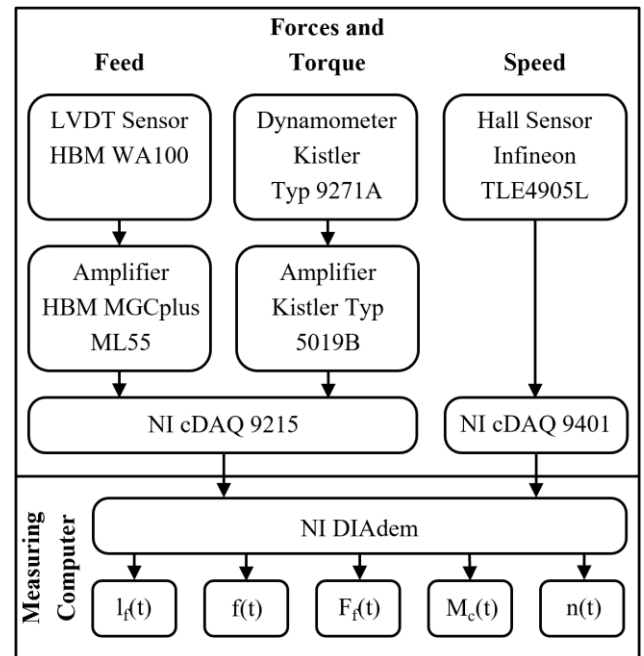


Fig 3. Measurement setup to determine time series data of the feed path $l_f(t)$, the feed $f(t)$, the feed force $F_f(t)$, the cutting torque $M_c(t)$ and the spindle speed $n(t)$

The spindle speed n is determined using a dedicated measurement setup consisting of a stationary stator ring with an integrated Hall-effect sensor and a rotating rotor ring containing two embedded permanent magnets for symmetry. The sensor employed is the Infineon TLE4905L, which incorporates an integrated Schmitt trigger. As the rotor magnets pass the sensor, magnetic field variations are converted into a digital HIGH/LOW output signal. This signal is acquired by a National Instruments NI 9401 cDAQ-module, which determines the signal period and converts it into a frequency. Based on the number of magnets embedded in the rotor, the frequency is converted into the spindle speed n in revolutions per minute within DAQmx. The feed motion or covered feed travel l_f of the drilling machine is captured using an inductive displacement sensor, which measures the relative distance between the machine and the workpiece during drilling. The recorded displacement data are differentiated in DAQmx to obtain the feed f . For this purpose, the difference between consecutive displacement values is divided by the sampling rate $f_s = 400$ Hz. The resulting signal exhibits significant noise. To mitigate this effect, two cascaded moving-average filters of window size $t_{win} = 0.125$ s are applied in DAQmx. In parallel, the unfiltered raw data are retained for subsequent detailed analyses. The feed force F_f and cutting torque M_c about the drilling axis are measured using a two-component dynamometer. Each dynamometer channel outputs an analog signal that is amplified by a Kistler 5019B charge amplifier to a ± 10 V signal and recorded via an NI 9215 cDAQ module. As with the displacement measurements, all signals are

transmitted to the measuring computer via an Ethernet interface for further processing and storage. Data acquisition is controlled by a trigger condition that initiates recording only when both the measured spindle speed n and feed force F_f exceed predefined threshold values. Because the drilling machine accelerates rapidly, the rotational speed threshold was deliberately set to a relatively high value of 80% of the nominal spindle speed to ensure that recording begins only under stable operating conditions, thereby enhancing the reliability of the acquired data. The start of the drilling must be carried out at the nominal speed.

3. Experimental procedures

To demonstrate the feasibility of the presented approach, initial manual drilling tests were carried out using the described test rig. A handheld electric drill was employed for this purpose, specifically the Atlas Copco EBB16, which features a programmable speed controller. During all trials, the spindle speed was set to $n_{\text{exp}} = 4,500 \text{ min}^{-1}$. The operator worked in a comfortable, chest-height horizontal position. A drill guide ensured consistent alignment and perpendicularity, simulating typical manual drilling in aircraft assembly and representing the ergonomic conditions of 80–90% of handheld drilling operations. The workpiece material consisted of Hexply M21/34%/UD194/IMA-12K, approximately $b = 5 \text{ mm}$ thick, with a glass-fiber layer on the exit side. Two identical uncoated cemented carbide sickle-type drill with a tool diameter of $D_t = 4.1 \text{ mm}$ were used that were new at the start of the experiments and worn out throughout the course of the experiments. 106 holes were drilled by a single operator with 9 holes being drilled by a second operator, resulting in a total of $N = 113$ holes. Three distinct feed-force levels were executed to ensure a dataset with high variability that could reasonably be found in a real production environment and study their respective influence on delamination at drill exit:

- Strong force – as high as the operator could reasonably apply ($F_f \approx 20 - 60 \text{ N}$),
- Medium force – firm but not maximal ($F_f \approx 10 - 40 \text{ N}$),
- Weak force – as low as possible while still enabling chip formation ($F_f \approx 5 - 30 \text{ N}$).

The sequence of tests was arranged in a random order to minimize systematic effects resulting from tool wear, operator fatigue or time of day. During drilling, all relevant process variables, which include feed force, torque, and feed motion, were recorded using the measurement setup described in the previous section. Experimental conditions like number of holes drilled, time-of-day and weekday were tracked. After drilling, the dimensionless delamination factor F_d at the exit was determined using an Olympus SZX10 stereomicroscope. The evaluation was carried out according to the method proposed by Davim et al in [16]. It is calculated using

$$F_d = \frac{D_{\text{max}}}{D_0} \quad (1)$$

with the maximum delamination diameter D_{max} and the hole diameter D_0 . Examples are shown in Fig 4.

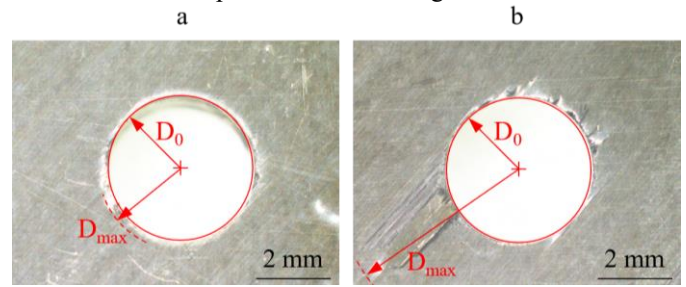


Fig 4. Example holes showing (a) good quality and (b) poor quality

4. Data Analysis

This section describes the systematical data analysis approach to determine the key influencing parameters on the exit layer delamination during manual drilling of CFRP.

4.1. Data labeling

A tolerance is defined on which labels separate the sample holes into two classes, as calculated in Eqn. 1. The first class, where the maximum delamination diameter D_{max} is in-tolerance and the second class where the maximum delamination diameter D_{max} is out-of-tolerance. The threshold value is defined as $F_d \leq F_{d,\text{max}}$ with the maximum delamination factor $F_{d,\text{max}} = 2$. This value was selected as a realistic and industry-comparable limit, ensuring the practical relevance of the investigated parameter range. Data labeling based on the threshold results in a dataset containing 25 out-of-tolerance samples (bad quality) and 88 within-tolerance samples (good quality), represented by a label vector $y \in \{1, 0\}^N$.

4.2. Feature extraction and data preparation

The data imported from the measurements are first processed using a moving average filter. The resulting timeseries data can be divided into two segments in order to analyze the influence of individual variables in specific phases of the drilling process. Segmentation is performed linearly with the first segment determining the first half of the drilling process and the second segment determining the second half according to the drilling time.

Tab 1. Feature examples (in total 32 features)

Name	Measurement	Segment	Symbol
max feed force seg. 1	F_f	1	$F_{f,1,\text{max}}$
min feed force seg. 2	F_f	2	$F_{f,2,\text{min}}$
mean feed total	f	total	f_{mean}
total drilling time	t	total	T
wear	-	-	N_t
...

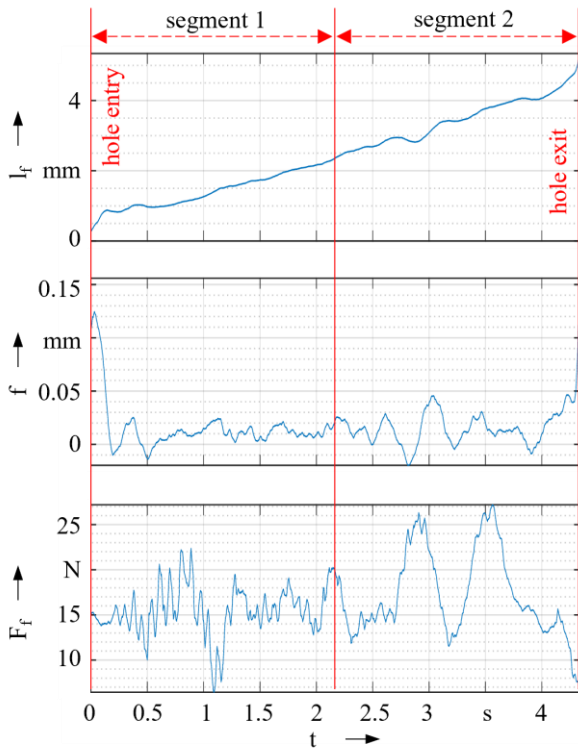


Fig 5. Time series data of a representative drilling process showing segmentation into drill entry and exit phases for feed path l_f , feed f , and feed force F_f

For each of the timeseries and additionally for each segment where applicable, characteristic parameters were extracted: the arithmetic mean, the maximum value, the minimum value and the slope over the entire series or segment. These values are then included as features for each drilling operation. Time of day and tool wear as the number of previous drilling operations N_t with this tool as well as spindle speed are also added. Finally, the total drilling duration is added as an additional feature leading to a feature vector x of length $p = 32$. An excerpt of some of the used features can be seen in Tab. 1. The features are calculated for all holes and stacked in a feature matrix $X \in \mathbb{R}^{N \times p}$. Fig. 5 shows the time series data of a representative manual drilling process. As described, the signal is segmented into segment 1 and segment 2 to capture the influence of the tool entry and exit phases, respectively. The feed path l_f exhibits noticeable variability, which is reflected in the non-constant feed f . In contrast to automated drilling with controlled feed motion, no distinct steady-state cutting phase can be observed. A comparison of feed force profiles for a new and a worn tool reveals a significantly higher variability when using the worn tool even within the same level of force, see Fig. 6. This suggests that maintaining stable feed control becomes more challenging for the operator as tool wear increases.

4.3. Feature Importance

To understand the correlations between the measurement process data and the hole quality a feature importance (FI) score is calculated. The FI score is a measure to quantify the importance that a specific feature has on the quality of the

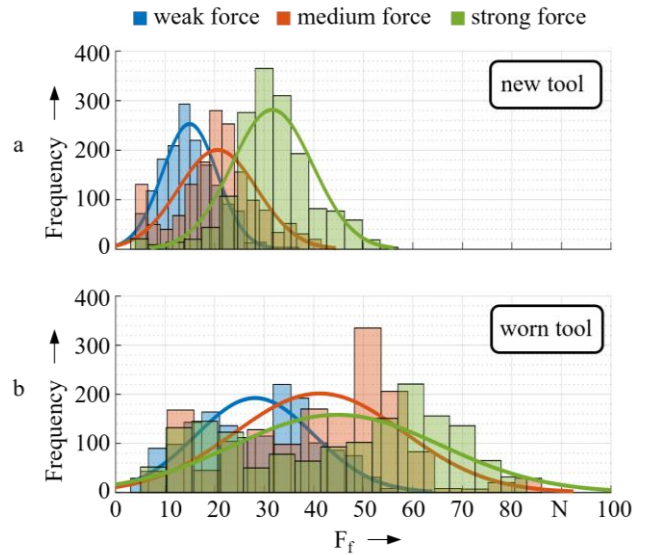


Fig 6. Histograms showing the force density of the feed force when drilling with subjectively weak, medium and strong force level for (a) a new tool (1-10 holes drilled per tool) and (b) a worn tool (40-50 holes drilled per tool)

prediction results. Several methods to determine the FI exist in the literature [17]. The calculation of the FI score can be regarded as a form of sensitivity analysis, as it assesses how changes in individual input features affect the model prediction outputs. In this study, the FI is determined using Random Forests and calculating the permutation importance, as show in Fig. 7. Compared to other feature relevance methods, the Random Forest with permutation importance provides a robust and model-agnostic measure that captures nonlinear interactions without requiring data normalization. Unlike

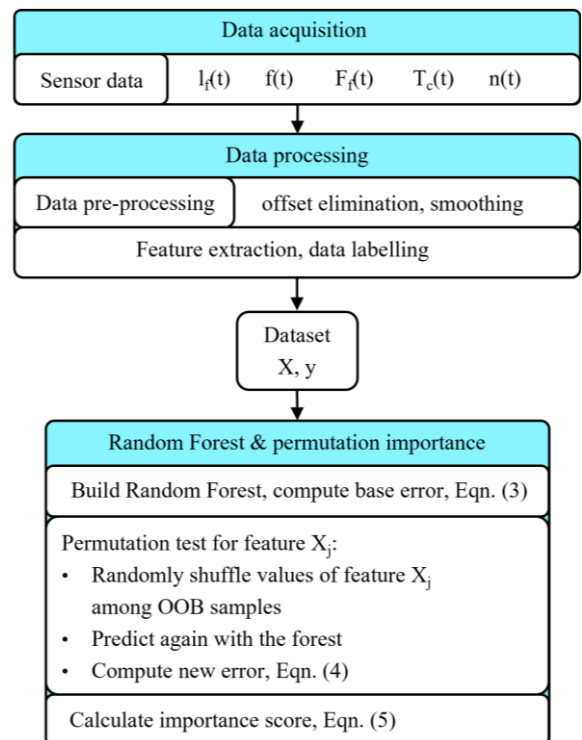


Fig 7. Flowchart of the presented feature importance method

purely statistical approaches such as correlation [18] or mutual information [19], this method directly quantifies the impact of each feature on the model's predictive performance, offering both convergence stability and interpretability. Using the permutation importance as importance score can alleviate the tendency of Random Forest to inflate the importance of numerical features [20] compared to categorical features. Based on the dataset with feature matrix X and label $y \in \{1, 0\}^N$, defining if the delamination factor F_d for a given hole i is below $y_i = 1$ or above $y_i = 0$ the threshold $F_{d,max}$, a Random Forest is constructed. A Random Forest is an ensemble of B decision trees $\{T_1, T_2, \dots, T_B\}$. In this case a number of decision trees $B = 200$ was used. Each tree is trained on a bootstrap sample, i.e., a random resampling with replacement of the training data. At each node, a random subset of the features is considered for splitting, which increases diversity and reduces overfitting. For a new observation x , the forest prediction \hat{y} is obtained via majority voting from the singular decision trees T_b as

$$\hat{y} = \text{mode}\{T_1(x), T_2(x), \dots, T_B(x)\}. \quad (2)$$

Due to bootstrap sampling, on average one third of the data is not included in the training set for each tree. These unused observations form the out-of-bag (OOB) set. Predictions on the OOB samples provide an unbiased estimate of the model's generalization error without requiring an explicit test set. Since each data point can be OOB multiple times across many trees, one obtains a statistically robust, quasi-stratified evaluation over the entire ensemble. The baseline OOB error E_{OOB} is computed as

$$E_{OOB} = \frac{1}{N_{OOB}} \sum_{i \in OOB} \{\hat{y}_i \neq y_i\}, \quad (3)$$

with the number of samples excluded from the bootstrap sample for a given tree N_{OOB} and the predicted and true label \hat{y} and y_i . For the current model, the baseline out-of-bag (OOB) error is $E_{OOB} = 0.23$, reflecting a reasonable level of generalization performance considering the inherent variability of manual drilling processes. To quantify the relevance of a select feature X_j , the following steps are performed: First, the values of X_j are randomly permuted within the OOB samples, destroying any relationship between X_j and the target label y . Second, the modified dataset is evaluated with the Random Forest, and a new OOB error is computed as

$$E_{OOB}^{(j)} = \frac{1}{N_{OOB}} \sum_{i \in OOB} \{\hat{y}_i^{(j)} \neq y_i\}. \quad (4)$$

Finally, the importance score for feature X_j is defined as the increase in prediction error. The increase in prediction error I_j for the j -th bootstrap sample is computed as

$$I_j = E_{OOB}^{(j)} - E_{OOB}, \quad (5)$$

with the difference between the new OOB error $E_{OOB}^{(j)}$ and the baseline error E_{OOB} . Features with large I_j values are critical for accurate classification, whereas features with small or negative values have little or even detrimental impact. Finally, the features are ranked according to their importance scores $\{I_1, I_2, \dots, I_p\}$.

4.4. Results

The developed Random Forest model was trained to identify the most influential process parameters affecting exit-layer delamination during manual drilling. The dataset comprised 113 samples with an imbalanced class ratio of approximately 1:3 between good and bad quality holes. Despite the limitation of the dataset, the model achieved a robust generalization performance, as indicated by the out-of-bag (OOB) results.

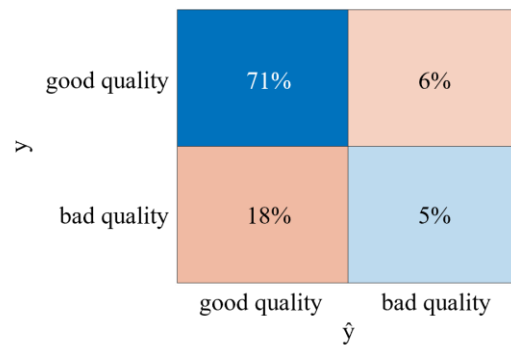


Fig 8. Confusion matrix showing true positives, false negatives, false positives and true negatives of the trained Random Forest classifier

The confusion matrix in Fig. 8 suggests that the model tends to favor correct identification of in-tolerance holes while still maintaining sensitivity toward delamination cases even though a clear bias is visible. The resulting OOB accuracy of 76 % confirms that the Random Forest effectively captures the dominant process relationships despite the small and imbalanced dataset. The ranked feature importance scores I_j in Tab. 2 reveal that the most influential predictors are kinematically related to feed motion and feed force, particularly during the exit phase (segment 2). The transverse fiber force acting perpendicular to the laminate plane, which can be approximated by the feed force F_f , is known from literature to be a decisive factor for delamination onset. The five most important features: maximum feed in segment 2 $f_{2,max}$, maximum feed force in segment 2 $F_{f,2,max}$, slope of total drilling time T_{slope} , slope of feed force $F_{f,slope}$ and total drilling time T , all directly or indirectly reflect this theoretical relationship.

Tab 2. Top 5 most important features

Rank	Name	Symbol	I_j
1	max feed seg. 2	$f_{2,max}$	0.31
2	min feed force seg. 2	$F_{f,2,max}$	0.29
3	slope total drilling time	T_{slope}	0.25
4	slope total feed force	$F_{f,slope}$	0.23
5	total drilling time	T	0.22

The boxplot in Fig. 9 illustrates the relationship between the maximum feed force in segment 2 and the delamination behavior, comparing new and used tools. For lower feed forces the delamination factor is lower for manual drilling, which corresponds to the results from automatic drilling of CFRP in the literature [8]. Additionally, this figure underlines the difficulty of high variability that is inherent to the manual drilling process. Furthermore, a clearer separation between the two delamination classes is observed for new tools, indicating more stable feed conditions and reduced force variability, which matches the overall feed force measurements in Fig 5. Therein could be observed, that higher tool wear leads to a higher degree of variability in the force measurement. In contrast, used tools exhibit higher scatter in feed forces, likely due to increased friction and reduced cutting efficiency, both of which contribute to higher delamination tendencies. Overall, these findings confirm that force- and feed-related quantities in the exit phase are the most relevant indicators of delamination. The insights gained provide a foundation for developing adaptive feedback systems for manual drilling, enabling real-time monitoring and potential process optimization based on feed force signals.

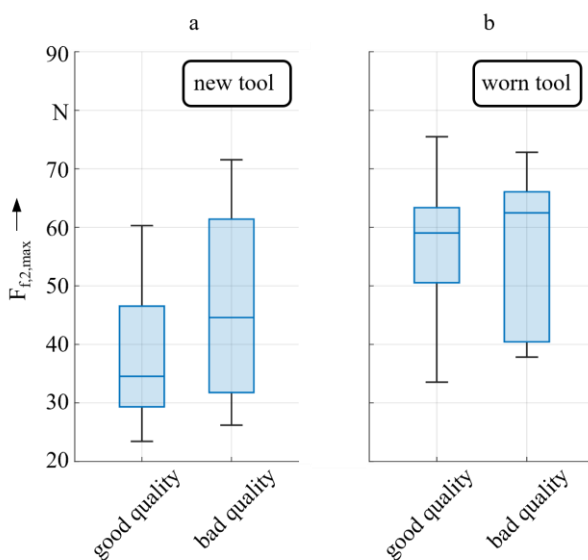


Fig 9. Boxplot of hole quality versus maximum feed force in segment 2. A clearer correlation tendency is observed for (a) the new tool (1-10 holes drilled per tool) than for (b) the worn tool (40-50 holes drilled per tool).

5. Conclusion and Outlook

Manual drilling remains a challenging process due to the strong influence of operator variability and multiple external factors such as worker experience, dexterity, fatigue and tool wear. To address these challenges, an experimental test rig was developed, equipped with external sensors for monitoring key process parameters, including feed force, cutting torque, feed travel, and spindle speed. The feed rate was additionally derived from these measurements. Based on the investigations into the manual drilling of CFRPs, several conclusions can be drawn:

- A correlation tendency exists between delamination and both feed rate and feed force during the hole exit phase, with higher feed rates and forces leading to increased delamination during manual drilling. This relationship, which is also affected by the total drilling time in the exit phase, aligns with current state-of-the-art findings in automated drilling [8] and the theoretical framework of the Kienzle equation [21], highlighting the interdependency between feed rate, feed force, and drilling time. Other external factors, such as time of day or weekday, did not show a significant influence on hole quality. A training effect for the machine operator during the experiments was not investigated.
- The variability in manual drilling data remains a major challenge. Feed force fluctuations exceeding 20 N were observed within a single drilling operation, depending on the operator. This variability significantly affects the statistical descriptors, such as the standard deviation and extreme values (min/max) and is dependent on the tool wear state.
- The Random Forest analysis further supports the experimental observations, highlighting that the most relevant features for predicting delamination are force- and feed-related quantities during the exit phase. Even though the absolute predicting ability of the model is limited, these findings underline the physical link between dynamic process forces and the occurrence of delamination damage.

Future studies will include a larger number of drilling experiments to improve statistical reliability and model robustness. The extended and more balanced dataset will enable a deeper understanding of the manual drilling process and support the development of an integrated operator feedback system for process stabilization. Moreover, the acquired data can serve as a foundation for anomaly detection applications, such as tool wear and breakage monitoring, ultimately contributing to enhanced process reliability and quality assurance in manual drilling.

References

- [1] Airbus. Airbus Global Market Forecast 2025-2044. Presentation; <https://www.airbus.com/sites/g/files/jlcbta136/files/2025-06/Presentation%20GMF%202025-2044.pdf>
- [2] Timmis AJ., Hodzic A, Koh L et al. Environmental impact assessment of aviation emission reduction through the implementation of composite materials. *Int J Life Cycle Assess* 2015, 20:233–243.
- [3] Al-Lami A, Hilmer P, Sinapius M. Eco-efficiency assessment of manufacturing carbon fiber reinforced polymers (CFRP) in aerospace industry. *Aerosp. Sci. Technol.* 2018, 79:669–678.
- [4] Hintze W. *CFK-Bearbeitung: Trenntechnologien für Faserverbundkunststoffe und den hybriden Leichtbau*. 1. Aufl. Berlin: Springer-Verlag, 2021. *german*
- [5] Araujo AC, Landon Y, Lagarrigue P. Smart drilling for Aerospace Industry: state of art in research and education, *Procedia CIRP* 2021, 99:387-391
- [6] Gao Y, Yang X, Xiao J et al. The development of an ultrasonic vibration hand-held pneumatic drill for hole-machining on CFRP composite materials. *Int J Adv Manuf Technol* 2021, 114:1635–1652.
- [7] Xu J, Geier N, Shen J, Krishnaraj V, Samsudeensadham S. A review on CFRP drilling: fundamental mechanisms, damage issues, and approaches toward highquality drilling, *J. Mater. Res. Technol.* 2023, 24:9677-9707.

- [8] Davim JP, Reis P. Study of delamination in drilling carbon fiber reinforced plastics (CFRP) using design experiments, *Composite Structures* 59 2003, 4:481-487.
- [9] Eneyew E, Ramulu M. Experimental study of surface quality and damage when drilling unidirectional CFRP composites. *Journal of Materials Research and Technology* 2014, 3:354-362.
- [10] Xu J, An Q, Chen, M. A comparative evaluation of polycrystalline diamond drills in drilling high-strength T800S/250F CFRP. *Composite Structures* 2014, 117:71–82.
- [11] Feito N, López-Puente J, Santiuste C, Miguélez MH. Numerical prediction of delamination in CFRP drilling *Compos Struct* 2014 108:677-683, 10.1016/j.compstruct.2013.10.014
- [12] Karnik S, Gaitonde V, Rubio JC, Correia AE, Abrão A, Davim JP. Delamination analysis in high speed drilling of carbon fiber reinforced plastics (CFRP) using artificial neural network model. *Mater Des* 29 2008, 9:1768-1776
- [13] Choi JG, Kim DC, Chung M, Lim S, Park HW. Multimodal 1D CNN for delamination prediction in CFRP drilling process with industrial robots. *Comput Ind Eng* 190 2024, Article 110074.
- [14] Hintze W, Hartmann D. Modeling of delamination during milling of unidirectional CFRP. *Procedia CIRP* 2013, 8:444-449
- [15] Su F, Zeng Z, Chen K, Che Y. Research on portable force-controlled machining device of CFRP and the method of thrust force controlling. *J Manuf Process* 2024, 131:781-796, 10.1016/j.jmapro.2024.09.072.
- [16] Davim JP, Rubio JC, Abrao AM. A Novel Approach Based on Digital Image Analysis to Evaluate the Delamination Factor After Drilling Composite Laminates. *Composites Science and Technology* 2007, 67:1939–1945.
- [17] Ewald FK, Bothmann L, Wright MN, Bischl B, Casalicchio G, König G. A Guide to Feature Importance Methods for Scientific Inference. In: Longo L, Lapuschkin S, Seifert C (eds) *Explainable Artificial Intelligence. xAI 2024. Communications in Computer and Information Science*, vol 2154. Springer, Cham.
- [18] Baba K, Shibata R, Sibuya M. Partial correlation and conditional correlation as measures of conditional independence. *Aust. New Zealand J. Stat.* 46 2004, 4:657–664.
- [19] Cover TM. *Elements of Information Theory*. Wiley; 1999
- [20] Breiman L. Random Forests. *Machine Learning* 45, 5–32; 2001.
- [21] Toenshoff HK. Cutting Tools. In: Chatti S, Laperrière L, Reinhart G, Tolio T, (eds) *CIRP encyclopedia of production engineering* 2019. Springer, Berlin.